Science of the Total Environment 583 (2017) 81–87

Contents lists available at ScienceDirect

Science of the Total Environment

journal homepage: www.elsevier.com/locate/scitotenv

Net deposition of mercury to the Antarctic Plateau enhanced by sea salt

Yeongcheol Han [a,b,*], Youngsook Huh [b], Soon Do Hur [a], Sungmin Hong [c], Ji Woong Chung [a], Hideaki Motoyama [d]

[a] Korea Polar Research Institute, 26 Songdomirae-ro, Yeonsu-gu, Incheon 21990, Republic of Korea
[b] School of Earth and Environmental Sciences, Seoul National University, 1 Gwanak-ro, Gwanak-gu, Seoul 08826, Republic of Korea
[c] Department of Ocean Sciences, Inha University, 100 Inha-ro, Nam-gu, Incheon 22212, Republic of Korea
[d] National Institute of Polar Research, 10-3, Midori-cho, Tachikawa-shi, Tokyo 190-8518, Japan

HIGHLIGHTS

- Sub-annual variations in Hg deposition were reconstructed from Dome Fuji snowpack.
- Cold vapor ICP-SFMS was applied to resolve a difference of sub-pg Hg g^{-1}.
- Increased concentrations of Hg and Na^+ were near-synchronous.
- A significant correlation was found between their annual deposition fluxes.
- Sea salt can control the net Hg deposition to the Antarctic Plateau.

GRAPHICAL ABSTRACT

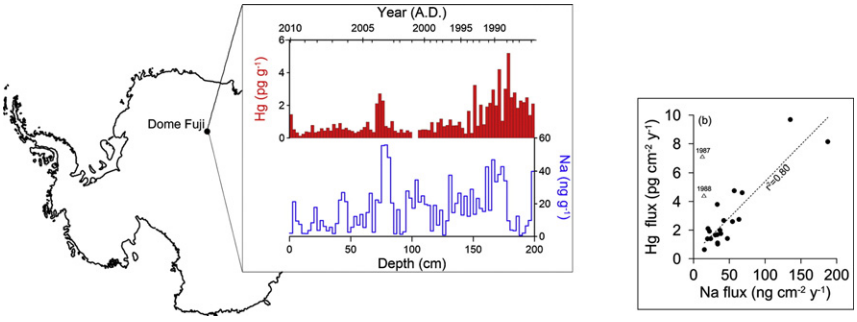

ARTICLE INFO

Article history:
Received 13 October 2016
Received in revised form 1 January 2017
Accepted 2 January 2017
Available online 23 January 2017

Editor: D. Barcelo

Keywords:
Photochemistry
Global Hg cycle
Antarctic snow
Sequestration
Oxidation
Reduction

ABSTRACT

Photochemically driven mercury (Hg) exchange between the atmosphere and the Antarctic Plateau snowpack has been observed. An imbalance in bidirectional flux causes a fraction of Hg to remain in the snowpack perennially, but the factors that control the amount of Hg sequestered on the Antarctic Plateau are not fully understood. We analyzed sub-annual variations in total Hg (Hg_T) deposition to Dome Fuji over the period of 1986–2010 using cold vapor inductively coupled plasma mass spectrometry and compared concentrations with those of sea salt components (Na^+ and Cl^-). Hg_T ranged from 0.12 to 5.19 pg g^{-1} ($n = 78$) and was relatively high when the Na^+ concentrations were high in the same or underlying snow layers. A significant correlation ($r = 0.7$) was found between the annual deposition fluxes of Hg_T and Na^+. Despite different origins and behavior of Hg and sea salt, the near-synchronous increases in the concentrations and correlation between the fluxes suggest that sea salt can intervene in the air-snow Hg exchange and promote the net deposition of Hg in the Antarctic Plateau.

1. Introduction

The Antarctic Plateau snowpack has been used for reconstructing past variations in global atmospheric background levels of trace metals (Boutron, 1995; Hong et al., 2012; Soyol-Erdene et al., 2011). In general, trace metal concentrations in Antarctic Plateau snow are considered dependent on their atmospheric loads, but recent studies have revealed that mercury (Hg) concentrations are primarily controlled by photochemical redox reactions (Angot et al., 2016; Brooks et al., 2008a). This is firstly because gaseous elemental Hg (Hg^0), the predominant form of Hg in the Antarctic atmosphere, weakly interacts with snow (Bartels-Rausch et al., 2008; Ferrari et al., 2004). The oxidized form (Hg^{II}) is highly reactive and easily adsorbed by snow. Thus, the oxidation of atmospheric Hg^0 to Hg^{II} leads to Hg deposition and can increase

* Corresponding author at: Korea Polar Research Institute, 26 Songdomirae-ro, Yeonsu-gu, Incheon 21990, Republic of Korea.
E-mail address: yhan@kopri.re.kr (Y. Han).

http://dx.doi.org/10.1016/j.scitotenv.2017.01.008
0048-9697/

Hg concentrations in surface snow up to hundreds of pg g^{-1} (Brooks et al., 2008a; Dommergue et al., 2010). Such surficial enrichment of Hg is usually transient, because most of the deposited Hg^{II} is photochemically reduced back to Hg^0 and returned to the atmosphere (Han et al., 2014). Only a fraction of Hg remains in snow over the course of the air-snow Hg exchange. As a footprint of the Hg exchange, this fraction is essential for investigating the factors affecting the bidirectional Hg flux (Sherman et al., 2010). Moreover, this fraction is destined for perennial sequestration in deep snow and ice (Brooks et al., 2008a; Jitaru et al., 2009). These temporary and perennial Hg fluxes can be important components of the global Hg cycle due to the vast extent (>5 million km^2) of the Antarctic Plateau (Brooks et al., 2008a).

In the Antarctic Plateau, a few studies have reported high total Hg concentrations (Hg_T) in surface snow driven by the oxidation of atmospheric Hg^0 during the summer. Brooks et al. (2008a) observed high Hg_T in the top layer of a snow pit (198 pg g^{-1}) and drifting snow (84 pg g^{-1}) at the South Pole. Comparable values were reported from near Dome C (4.2–194 pg g^{-1}; Dommergue et al., 2012). Although the elevations were less at Dome A (0.2–8.3 pg g^{-1}; Li et al., 2014) and Dome Fuji (<0.4–10.8 pg g^{-1}; Han et al., 2011), Hg_T concentrations in the surface snow were still higher than those in snow pits (0– < 4 m in depth); this is consistent with the summertime enhancement of Hg deposition (Han et al., 2014; Li et al., 2014). The difference of the surficial Hg_T among the sites may indicate a spatio-temporal heterogeneity of Hg dynamics over the vast Antarctic Plateau, spatial variation in snow accumulation, inconsistent sampling thickness for surface snow and different analytical methods (Han et al., 2014).

How the surface snow becomes enriched with Hg during the summer is still uncertain. A central question has been what oxidizes atmospheric Hg^0 to Hg^{II} and consequently promotes Hg deposition. In coastal/sea ice regions, marine halogens derived from nearby sea ice have been identified as major oxidants leading to Hg^0 oxidation, rapid deposition of Hg^{II}, and atmospheric Hg depletion (Brooks et al., 2008b; Nerentorp Mastromonaco et al., 2016). Marine halogens have been proposed to play the same role in the Antarctic Plateau (Brooks et al., 2008a). However, minimal amounts of marine halogens can reach the remote inland (Hara et al., 2004; Suzuki et al., 2002) and even less during the summer when photochemistry is active (Hara et al., 2004). Even if marine halogens are the major oxidants in the Antarctic Plateau, the potential relationship between the halogen and Hg concentrations in snow is liable to disappear due to the post-depositional behavior of Hg (Dommergue et al., 2012; Han et al., 2014). For example, the slow snow accumulation at Dome Fuji (~8 cm y^{-1}) allows ample time for the photochemical reduction and re-emission of the deposited Hg, when an effective sunlight penetration depth of >10 cm under dry snow conditions is considered (King and Simpson, 2001). Influences of non-halogen radicals (e.g., OH, NO_2 or HO_2; Angot et al., 2016) on the Hg^0 oxidation can be another obstacle to revealing the relationship between the halogen and Hg concentrations in snow.

Despite re-emission, a fraction of Hg is perennially sequestered in the snowpack. The Hg sequestration rate varies with atmospheric and snow conditions that regulate the bidirectional Hg flux (Durnford and Dastoor, 2011). Accordingly, reconstruction of the temporal variation in Hg sequestration can contribute to understanding past environmental conditions. For instance, the Hg sequestration rate was substantially higher under the dusty conditions of the glacial period (121 pg cm^{-2} yr^{-1}; Jitaru et al., 2009) compared to the present (<3 pg cm^{-2} y^{-1}; Han et al., 2014); the higher sequestration rate was attributed to dust particles behaving as a scavenger of atmospheric Hg^{II} and a stabilizer of particle-bound Hg^{II} against re-emission (Jitaru et al., 2009).

Measuring the low concentrations of Hg_T in the Antarctic Plateau snow requires a precise analytical technique. Previously, ICP-SFMS (inductively coupled plasma sector field spectrometry) performed comparably to the conventional cold vapor (CV) generation method (e.g., CV atomic fluorescence spectrometry) (Planchon et al., 2004). Less sample consumption is an advantage of using ICP-SFMS, which is especially important when sample volume is limited (Han et al., 2011; Jitaru et al., 2009). However, signal-to-background ratio and instrumental sensitivity were insufficient to resolve a difference of sub-pg g^{-1} for Antarctic snow samples (Han et al., 2014). Therefore, we adopted CV-ICP-SFMS for more precise determination of the Hg contents in Antarctic Plateau snow. Using the CV system improved the signal-to-background ratio by up to a factor of 10.

CV-ICP-SFMS was applied to a Dome Fuji snow pit, with samples collected every 2.5 cm from the surface down to a depth of 2 m. Because the sampling interval (2.5 cm) was equivalent to approximately one-third of the annual snow accumulation at Dome Fuji (< ~ 10 cm as snow; Kameda et al., 2008), the temporal variation in the snow composition could be investigated on a sub-annual scale. We compared Hg_T with the Na^+ and Cl^- concentrations and $\delta^{18}O$ to examine the interrelations between them and evaluated the temporal variation in Hg deposition. We expect this study to contribute to the understanding of the dynamics of Hg in the Antarctic Plateau and its role in the global Hg cycle.

Recently, research based on year-round monitoring of atmospheric Hg has been reported from Antarctic inland sites (Angot et al., 2016; Pfaffhuber et al., 2012). Those studies observed significant variations of atmospheric Hg^0 on diurnal to seasonal time scales resulting from active photochemical interactions between the atmosphere and the snowpack. Our results can give a clue to the connection between the short-term variations in atmospheric Hg and the resulting variations in snowpack Hg concentrations on sub-annual to multi-year scales.

2. Materials and methods

2.1. Sample description

A snow pit was excavated at a site (77.39°S, 39.62°E, 3790 m) near Dome Fuji in East Antarctica on January 21, 2010, during the 51st Japanese Antarctic Research Expedition (Fig. 1). Snow samples were collected from the surface down to a depth of 2 m by inserting a Teflon cylinder (I.D. 2.5 cm) horizontally into the pit wall. The snow from each layer was separated into two containers: a 125 mL PFA bottle for the analyses of Hg and Ba, and a 1 L LDPE bottle for the analyses of stable oxygen isotopes ($\delta^{18}O$) and major ions (Na^+, Cl^- and SO_4^{2-}). The sample bottles were double-sealed in acid-cleaned LDPE bags and were kept

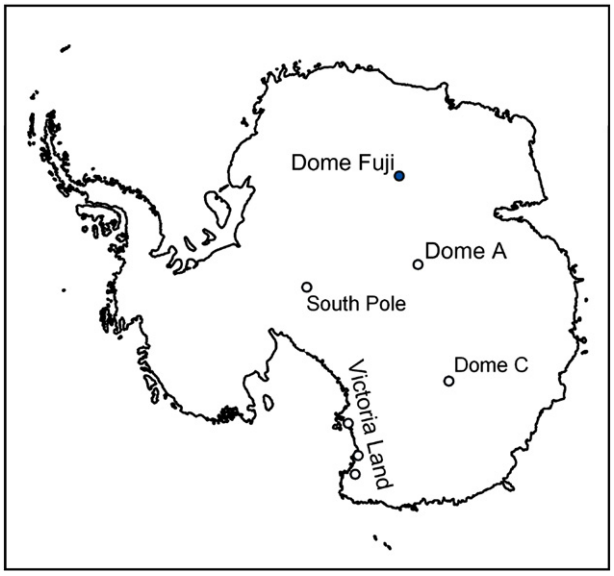

Fig. 1. The sampling location for the 2 m deep Dome Fuji snow pit (closed circle). The sites for the studies cited in the text are also indicated (open circle).

frozen in the dark until further processing. Two PFA bottles for the depth interval of 100–105 cm were lost during transport. All sampling items were prepared at the Korea Polar Research Institute (KOPRI) following the cleaning procedure described by Hong et al. (2000).

2.2. Sample preparation

Snow samples contained in the PFA bottles were melted at room temperature in a class 100 clean hood and aliquoted into two 8 mL Teflon-lined glass vials (Wheaton) that were pre-cleaned following US EPA method 245.7 (US EPA, 2005). One vial was immediately analyzed, and the other was digested overnight with 0.5% (v/v) BrCl before analysis. The latter recovered the total Hg (Hg_T) in the snowmelt, and the former measured the labile fraction of Hg_T readily reduced within the CV generator without the pre-oxidation step (Hg_L, hereafter). The amounts of sample and added BrCl were weighed to correct for any Hg impurities in the BrCl. The procedural blank using DI water was below the detection limit (0.03 pg g^{-1}).

2.3. Instrumentation

Mercury concentrations were determined using CV-ICP-SFMS at the National Center for Inter-University Research Facilities at Seoul National University. An Element2 mass spectrometer (Thermo Finnigan, Germany) was coupled with a CV generator (HGX-200, Cetac, USA) as a sample introduction system. In the CV generator, Hg^{2+} in the sample solution was reduced to Hg vapor (Hg^0) by 4% (m/v) $SnCl_2$ and transferred into the ICP via a liquid-vapor separator. Hence, the CV system could minimize potential isobaric interference of polyatomic species on Hg (e.g., $^{186}W^{16}O$ on ^{202}Hg) by selectively transferring Hg vapor into the plasma. The sample consumption rate was ~1 mL min^{-1}, and ~3 mL was used for triplicate analysis of each sample (5 runs × 9 passes for a single analysis). The Element2 parameters were optimized for maximum performance prior to sample analysis.

Working standard solutions for external calibration were prepared by sequential dilution of a single elemental standard of Hg at 1000 mg L^{-1} in a 10% HNO_3 matrix (ICP standard, Merck) to the range of 0–50 pg g^{-1}. Hg in the standard solutions was preserved with 0.5% (v/v) BrCl (US EPA, 2005). Instrument sensitivity indicated by the slopes of the calibration curves were ~1800 cps (counts per second) pg^{-1} g for ^{202}Hg ($r^2 > 0.9999$) and ~800 cps pg^{-1} g for ^{201}Hg ($r^2 > 0.9999$). The accuracy of the calibration curve was verified by analyzing the certified reference material ORMS-4 (elevated Hg in river water, 22.0 ± 1.6 pg g^{-1} stabilized with 0.5% (v/v) BrCl, NRCC), which showed a good recovery of 21.2 ± 1.0 pg g^{-1} (standard deviation, n = 6). Detection limits, estimated as three times the standard deviation of the blank signal (n = 9), were 0.03 pg g^{-1} and 0.04 pg g^{-1} for ^{202}Hg and ^{201}Hg, respectively. External reproducibility, which was 5.4% (relative standard deviation, n = 20) over the course of the analysis, was evaluated using a 5 pg g^{-1} standard solution. The external reproducibility is further examined by aliquoting a snowmelt sample into three separate vials. The mean reproducibility for the samples containing 0.4–3 pg Hg_T g^{-1} (n = 5) and 0.03–0.75 pg Hg_L g^{-1} (n = 5) was 2.5% and 14%, respectively.

Oxygen isotope ratios ($\delta^{18}O$) and major ion concentrations (Na^+, Cl^- and SO_4^{2-}) of the snowmelt were determined at KOPRI using cavity ring-down spectroscopy (L1102-i, Picarro, USA) and ion chromatography (ICS-2000, Dionex, USA), respectively. The external reproducibility, shown as standard deviation, was better than 0.08‰ and 5%, respectively. Barium concentrations were measured for the samples below a depth of 135 cm using ICP-SFMS at KOPRI with a micro-flow nebulizer and a cyclonic spray chamber (Elemental Scientific, USA) as a sample introduction system. The detection limit was 4.7 pg g^{-1}, and the external reproducibility was 5.4% (n = 4).

2.4. Reagents and blanks

BrCl and $SnCl_2$ solutions were prepared based on US EPA method 245.7 (US EPA, 2005). The BrCl solution was prepared immediately prior to use by mixing a bromate/bromide solution and concentrated hydrochloric acid (HCl, Optima grade, Fisher) (1:1 v/v). To produce the bromate/bromide solution, 2.78 g of $KBrO_3$ (ACS reagent, ≥99.8%, Sigma-Aldrich) and 11.90 g of KBr (ACS reagent, ≥99.0%, Sigma-Aldrich) were preheated at 250 °C for >8 h to volatilize the Hg impurities and were dissolved in 500 mL of deionized water (DI water). The Hg impurities in the BrCl solution were 28.1 ± 7.5 pg g^{-1} (n = 7), equivalent to 0.14 ± 0.03 pg g^{-1} in the sample solution when added to a final concentration of 0.5% (v/v). A 4% (w/v) $SnCl_2$ solution (reagent grade, 98%, Sigma-Aldrich), used as the reducing agent in the CV generator, was prepared in 3% (v/v) HCl (HP-100H, Eco Research) and purged with pure N_2 gas (>99.9999%) for 30 min to eliminate trace Hg in solution.

The Hg concentration in the DI water was below the detection limit (0.03 pg g^{-1}) and was indistinguishable from DI water purged with $SnCl_2$. The background signal was monitored by analyzing DI water between each sample and was subtracted from the signals of the samples.

3. Results and discussion

3.1. Variation in the Hg concentration with depth

The Hg concentrations with (Hg_T) and without (Hg_L) the BrCl pretreatment steps ranged from 0.12 to 5.19 pg Hg_T g^{-1} and from <0.04 to 1.83 pg Hg_L g^{-1} (n = 78), respectively (Fig. 2a; Table S1). They were all within the previous results for Antarctic snow (Durnford and Dastoor, 2011; Han et al., 2011). The mean Hg_L/Hg_T ratio was 0.22. This value was comparable to the 0.20–0.25 ratio found by comparing the results for Dome C ice core sections of similar ages (0–34 ka) from Jitaru et al. (2009) (Hg_T) and Vandal et al. (1993) (Hg_L). Early studies that determined Hg concentration without the pre-oxidation step (Vandal et al., 1993; Capelli et al., 1998) are expected to underestimate Hg_T by a factor of 4–5. Their relatively low results are then partly ascribed to the analytical method, suggesting that differences in analytical methods should be taken into account when comparing data. Although Hg_L were lower than Hg_T, we found a strong correlation between them (r = 0.91). Since inorganic Hg forms the majority of Hg_T in Antarctic inland snow/ice (Jitaru et al., 2009), the Hg_L in this study represents the readily reducible fraction of inorganic Hg, including the Hg ion (Hg^{2+}). We focus on Hg_T in the following discussion.

The variation in Hg_T displayed a marked transition across the depth of 140 cm; Hg_T was lower (0.7 pg g^{-1}; n = 54) and less variable (±0.5 pg g^{-1}; standard deviation) above 140 cm if two exceptional increases in the intervals of 0–2.5 cm and 70–77.5 cm are excluded (Fig. 2). In contrast, Hg_T was higher (2.2 pg g^{-1}; n = 24) and fluctuated (±1.2 pg g^{-1}) below 140 cm. The highest Hg_T (5.19 pg g^{-1}) occurred at depths of 177.5–180 cm.

3.2. Seasonality of $\delta^{18}O$ and the sea salt concentrations

Precipitation on the Antarctic Plateau has strong seasonality with high $\delta^{18}O$ in summer and low $\delta^{18}O$ in winter due to its dependency on air temperature where snow forms; this difference has been used to identify seasonal layers in the snowpack. $\delta^{18}O$ varied between −64‰ and −50‰ in our samples (Fig. 2e), comparable to the previous results for Dome Fuji snow pits (−63‰--49‰ in Hoshina et al. (2014); −62‰--45‰ in Iizuka et al. (2004)). This range was narrower than that of fresh snowfall (e.g., −82‰ (winter)--33‰ (summer) in 2003; Fujita and Abe, 2006), possibly due to post-depositional processes such as surface snow redistribution (Motoyama et al., 2005) and smoothing by isotopic diffusion (Hoshina et al., 2014). Nevertheless, the variation in $\delta^{18}O$ within the snowpack should be ascribed foremost to the climatology of seasonal precipitation.

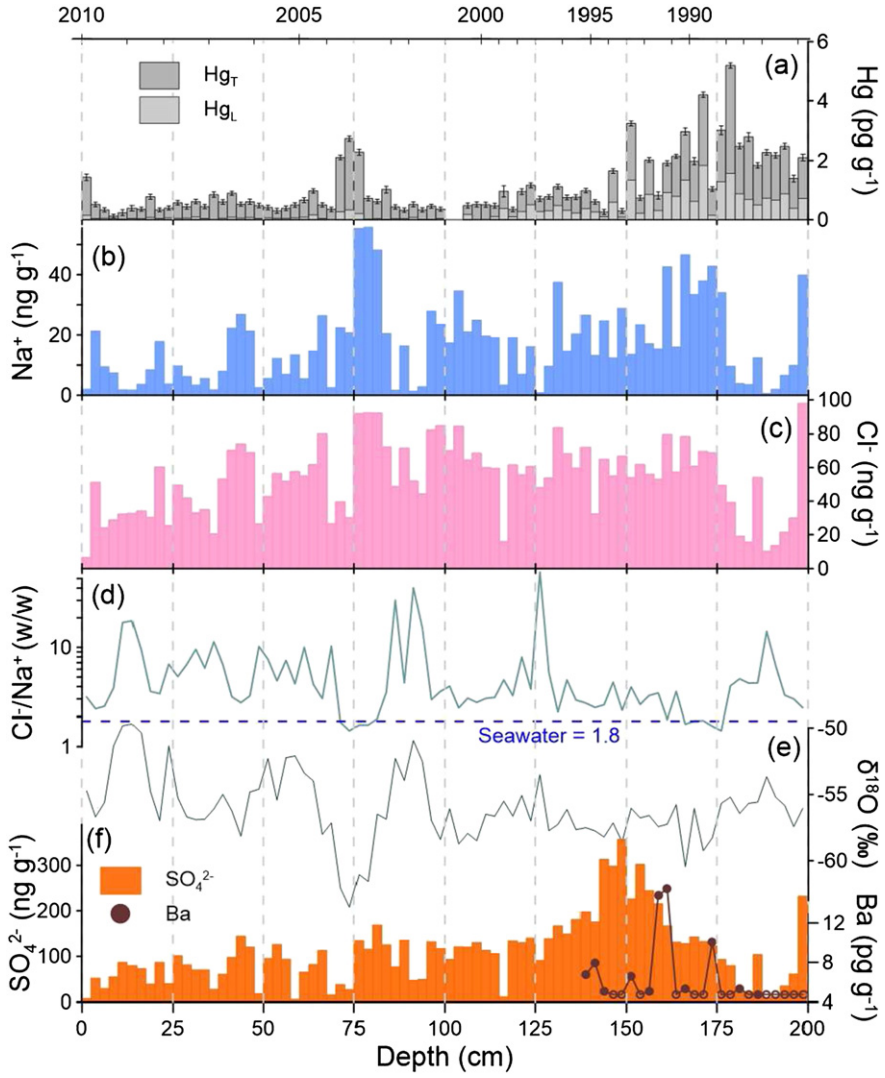

Fig. 2. The depth profiles of the (a) labile (Hg_L, pale bar) and total (Hg_T, dark bar with ±2 standard deviation error range) Hg concentrations, (b) Na^+ and (c) Cl^- concentrations, (d) Cl^-/Na^+ ratio (w/w), whose seawater value is 1.8, (e) $\delta^{18}O$, and (f) SO_4^{2-} (bar) and Ba (line with circles) concentrations. The Ba contents below the detection limit (4.7 pg g^{-1}) are shown as open circles. The age of snow is shown on the top x-axis.

The quantity of marine aerosols transported from the coastal regions to Dome Fuji exhibits a strong seasonal cycle with winter maxima and summer minima (Hara et al., 2004). Hence, the sea salt contents in the snowpack are an independent seasonal marker, although they also suffer from post-depositional alteration (Iizuka et al., 2004). We ascribed the variation in Na^+, ranging from 0.7 to 56 ng g^{-1}, to the winter-high and summer-low cycle of sea salt deposition (Fig. 2b) because at Dome Fuji, Na^+ in snow originates exclusively from sea salt and is less mobile after deposition relative to other sea salt components (Hara et al., 2004; Iizuka et al., 2004). The seasonality of Na^+ was further evidenced by its negative correlation with the Cl^-/Na^+ ratio ($r = -0.46$, $p < 0.001$; Fig. 2b–d). The Na-high winter layers had Cl^-/Na^+ ratios of ~1.8 (w/w) equivalent to the ratio of sea salts (Fig. 2d). In contrast, the ratio reached levels >50 in the Na-low summer layers due to both the low Na^+ content and the extra input of Cl^- (Suzuki et al., 2002). In the Antarctic Plateau, the excess Cl^- is not fully understood but has been ascribed to the fact that Cl^-, compared with Na^+, is preferentially liberated from marine aerosols, transported over long distances from coastal to inland regions and recycled after deposition (Hara et al., 2004; Iizuka et al., 2004, 2012). Excess Cl^- is more influential during the summer (Hara et al., 2004; Iizuka et al., 2004) and produces a seasonal Cl^-/Na^+ cycle in the snowpack.

A negative relationship was found between $\delta^{18}O$ and Na^+ ($r = -0.64$, $p < 0.001$). The consequent covariations of $\delta^{18}O$, Na^+ and Cl^-/Na^+ (Fig. 2b–e) indicate that their variations were primarily seasonal. Previously, such correlations were observed only on a multi-year scale at Dome Fuji (Hoshina et al., 2014; Iizuka et al., 2004). We expect that our sampling site was less disturbed post-depositionally than previous study sites.

The well-preserved seasonality is further supported by the snow depth-age relationship established based on a well-known volcanic sulfate peak and annual layer counting. The largest sulfate peak, found at a depth of 147.5 cm, has been attributed to the Mt. Pinatubo eruption in June 1991 and was assigned to early 1994 in consideration of the travel time of volcanic emissions (Fig. 2f) (Soyol-Erdene et al., 2011). The annual layer counting relying on the seasonality of $\delta^{18}O$ and Na^+ dated the Pinatubo peak also to 1994 (Fig. 2).

Based on the depth-age relationship and an empirical equation for snow depth (z in m)-density (ρ in kg m^{-3}) at Dome Fuji, $\rho(z) = 408 - 118\exp(-z/1.72)$ (Takahashi and Kameda, 2007), the mean snow accumulation rate was calculated to be 27.8 kg m^{-2} y^{-1}. This value agreed with the mean rate measured with bamboo stakes about 8 km away from our sampling site (27.3 ± 1.5 kg m^{-2} y^{-1}) during 1995–2006 (Kameda et al., 2008). However, if we select the depth interval of 0–140 cm (corresponding to 1995–2010), the rate increased to

30.3 kg m^{-2} y^{-1}; hence, a higher temporal resolution could be expected. Since annual precipitation monitored with the bamboo stakes did not increase since 1995 (Kameda et al., 2008), the snow accumulation at our sampling site must be locally high during the period and well preserved against redistribution of surface snow.

3.3. Seasonality of Hg_T and the potential role of sea salt

It is likely that variation in Hg_T is also seasonal. When compared with Na^+, the peaks of Hg_T tend to lag the Na-high layers by 0–5 cm (Fig. 2a–b). These lags are more obvious above 140 cm, where the temporal resolution is greater. For example, the Hg_T peaks at depths of 0–2.5, 17.5–20, 40–42.5, 62.5–65 and 70–77.5 cm commonly appear 2.5 cm above the Na-high layers. The lags are also present below 140 cm but are less clear due to poor temporal resolution. The Hg_T and Na^+ concentrations were determined from different portions of a horizontal snow layer contained in Teflon and polyethylene bottles, respectively. Therefore, we do not exclude the possibility that such a small depth lag was caused by an undulation of a snow layer of the same age (Kameda et al., 2008). Nevertheless, the Hg_T peaks should be associated with the winter season rather than the summer. The highest Hg_T peaks at depths of 70.0–77.5 cm and 160.0–177.5 cm occurred with the highest Na^+ concentrations (>60 ng g^{-1}), Cl^-/Na^+ ratios similar to that of sea salt (~1.8) and the lowest $\delta^{18}O$ (< −60‰), all characteristic of the winter layers. In order to quantitatively examine the timing of the Hg_T peak, seasonal mean variations of Hg_T, $\delta^{18}O$ and Na^+ concentration for the depth interval of 0–140 cm (corresponding to 1995–2010) are compared in Fig. 3. Annual maxima and minima of $\delta^{18}O$ are assumed to correspond to mid-summer (Jan) and mid-winter (Sep) (Fig. 3b), respectively, and Na^+ concentration and Hg_T are normalized to their annual mean values (Fig. 3a and c). Because of the negative correlation between $\delta^{18}O$ and Na^+, the winter-high and summer-low feature of Na^+ is well captured (Fig. 3c). When compared with Na^+, the Hg_T peak is shown to appear ~1.5 month after the mid-winter Na^+ peak. Therefore, we conclude that the Hg_T peak lies between the mid-winter and early summer layers.

The observation that the Hg_T peaks follow the Na^+ peaks raises questions about the role of sea salts in the redox chemistry of Hg. First, halogens released from sea salts could promote oxidation of atmospheric Hg^0 and subsequent Hg^{II} deposition as previously proposed (Brooks et al., 2008a). Then, the timing of the Hg_T peaks would reflect the most active Hg^0 oxidation immediately after the polar sunrise because of the abundant halogen supply from the surface snow enriched in sea salt during winter. However, year-round observations at Dome C and the South Pole revealed that the oxidation of atmospheric Hg^0 were more active in mid- (Nov–Dec) and late (Jan–Feb) summer than early summer (Sep–Oct), respectively (Angot et al., 2016; Brooks et al., 2008a). Second, sea salt could behave as stabilizing agents for Hg^{II} in snow. Assuming that sea salt particles play the same role as dust particles, Hg^{II} bound to sea salt grain can be stable against photochemical reduction (Jitaru et al., 2009). Alternatively, halides can be liberated from sea salt and form complexes with Hg^{II} (Hara et al., 2004). These complexes are relatively stable against photochemical reduction in snow and hence lessen Hg loss from the snowpack (Durnford and Dastoor, 2011; Mann et al., 2014). The stabilizing effect of sea salt can explain the simultaneously high concentrations of both Hg_T and Na^+. In addition, the lack of a Hg_T peak in the mid- to late summer layers (Fig. 3a) can be ascribed to the reduction of Hg^{II} in the absence of sufficient sea salt in the surface snow. If this is the case, it can be further inferred that the excess Cl abundant in summer (Fig. 2d) could not lessen Hg loss. The role of sea salt particles or other halides in sea salt (e.g., Br) might then be more effective for Hg stabilization.

The previous results at the South Pole suggested that the atmospheric Hg^{II} concentration peaked in late summer (Brooks et al., 2008a); another result at Dome C showed Hg_T in surface snow was highest in mid-summer (Angot et al., 2016). In contrast, Hg_T in the Dome Fuji snowpack reached a maximum between winter and early summer. If those observations are combined, it can be inferred that the Antarctic Plateau snowpack acts as a sink of Hg from mid-winter to mid-summer, with greater deposition than re-emission, but changes its role to a source of atmospheric Hg during mid- to late-summer, with greater re-emission than deposition (Fig. 3a). This inference is supported by the observation at Dome C that atmospheric Hg^0 concentrations gradually decreased in winter (from ~0.8 to ~0.6 ng m^{-3}) and was higher in late summer (>1.0 ng m^{-3} in 2012–13) than its annual mean (0.8 ng m^{-3} in 2012–13), implying Hg deposition in winter and greater re-emission from the snowpack than deposition in late summer (Angot et al., 2016).

3.4. What could influence the Hg sequestration rate in the Antarctic Plateau?

The mean sequestration rate of Hg was calculated to be 3.3 pg cm^{-2} yr^{-1} based on the depth-age relationship and the empirical depth-density equation. This rate was comparable to the interglacial rate at Dome C (~6 pg cm^{-2} yr^{-1}; Jitaru et al., 2009). When we simply apply this rate, the entire Antarctic Plateau is expected to sequester 0.2 t Hg a year, much lower than the previous estimation of 60 t Hg y^{-1} (Brooks et al., 2008a). We suggest this value as a lower limit because the Hg sequestration rate likely increases from inland to coastal (Han et al., 2014). The present rates at near-coastal sites in Victoria Land are 3.9–11 pg Hg_L cm^{-2} yr^{-1} (Capelli et al., 1998; Witherow and Lyons, 2008). If a Hg_L/Hg_T ratio of 0.22 is applied, those near-coastal sites would sequester up to 15 times more Hg than Dome Fuji. Our previous estimation at Dome Fuji was 1–2 pg cm^{-2} yr^{-1}. The lower result in our previous study was ascribed to the low signal-to-blank ratio of the analytical technique and not incorporating a preservative to protect against Hg loss from the sample (Han et al., 2014).

Sea salt deposition in the polar night is crucial to the annual net deposition of Hg, which is more convincing when the annual fluxes of Na^+ and Hg_T are compared (Fig. 4). Their fluxes are significantly correlated ($r = 0.70$ including the outliers in Fig. 4; $p < 0.001$). We propose that

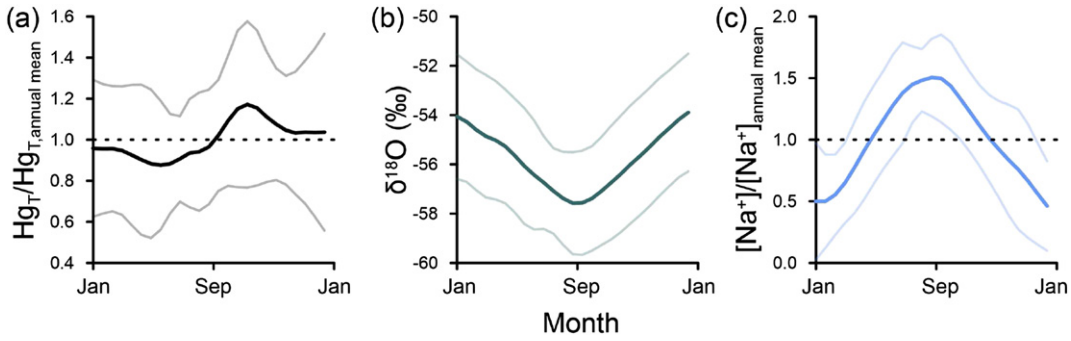

Fig. 3. Seasonal mean variations of (a) Hg_T, (b) $\delta^{18}O$ and (c) Na^+ for the depth interval of 0–140 cm (corresponding to 1995–2010). Hg_T and Na^+ concentration are normalized to their annual mean values. Each plot is shown with ±1 standard deviation error range.

although the photochemical processes in the summer lead to increased Hg content in snow, the sea salt flux in the preceding winter is more crucial to the Hg sequestration rate in the Antarctic Plateau.

The sea salt flux in the Antarctic Plateau is influenced by the emission intensity of the sources, the transport pathway and deposition efficiency (Hara et al., 2004; Udisti et al., 2012; Wolff et al., 2006). The production of sea salt aerosols is generally high in winter due to the larger extent of sea ice with frost flowers and blowing snow, which were indicated as more influential sources of sea salts than the open sea (Rankin et al., 2002; Yang et al., 2008), and strong wind conditions over the source regions (Hara et al., 2004). However, increases in sea salt aerosols at inland sites were episodic rather than persistent during the winter season (Hara et al., 2004; Udisti et al., 2012). Such episodic events could occur in association with synoptic-scale meteorological conditions, which provide efficient pathways for the sea salt transport from the coastal regions to the interior. For example, a blocking anticyclone renders efficient advection of warm and moist air masses with abundant marine aerosols and causes heavy snowfall with substantial sea salt deposition over a wide expanse of the Antarctic interior (Enomoto et al., 1998; Fujita and Abe, 2006; Massom et al., 2004; Schlosser et al., 2010). The thickest and highest Hg_T peaks at depths of 70.0–82.5 cm, concurrent with the highest Na^+ and the lowest $\delta^{18}O$ and Cl^-/Na^+, is the result of a heavy snowfall event associated with a blocking event in the winter season, unless it formed post-depositionally. The frequency of the blocking event would considerably affect the sea salt flux in the Antarctic Plateau. However, it seems to vary widely year-to-year (Schlosser et al., 2010), and observations are insufficient to address its long-term trend and its impact on the interannual Hg_T variation.

Over glacial-interglacial cycles on the Antarctic Plateau, sea salt flux is generally higher during the cold period than the warm period. At Dome Fuji, for example, the mean flux of sea salt Na^+ between the last glacial maximum and termination (11.7–20 ka) was 85 ng cm^{-2} y^{-1}, higher than 62 ng cm^{-2} y^{-1} since the last glacial termination (0–11.7 ka) (Iizuka et al., 2008). If we apply the regression line in the Fig. 4b, the mean Hg_T flux would be approximately 30% higher in cold periods (4.6 pg cm^{-2} y^{-1}) than in warm periods (3.5 pg cm^{-2} y^{-1}). The sea salt Na^+ fluxes were similar at Dome C, 83 ng cm^{-2} y^{-1} (13–19 ka) and 53 ng cm^{-2} y^{-1} (0–11 ka) (Wolff et al., 2006). However, the Hg_T flux varied between <2 and 15 pg cm^{-2} y^{-1} ($n = 9$) and was not obviously associated with the sea salt Na^+ flux during these periods (Jitaru et al., 2009), possibly due to the small sample numbers for Hg_T and their different temporal resolution with Na^+. When the entire records for the past 670 ka are taken into account, the Hg_T flux was greater during the cold periods (up to ~29 pg cm^{-2} y^{-1}) than during the warm periods (~6 pg cm^{-2} y^{-1}) (Jitaru et al., 2009). The greater flux in the cold periods was attributed to more abundant dust, which would stabilize Hg^{II} in the snow against re-emission (Jitaru et al., 2009). However, the sea salt flux was also greater during the cold periods, and our results suggest that the sea salt could play a role in Hg^{II} stabilization in snow. Further study of the Na^+ and Hg_T concentrations in the same samples could properly gauge the contribution of sea salt to the Hg_T flux in the past.

To examine the contribution of terrestrial dust to Hg sequestration, Ba concentrations as a proxy of terrestrial dust input were compared with Hg_T below 140 cm (Fig. 2f). The Ba contents were generally below the detection limit (4.7 pg g^{-1}) with a few sporadic peaks. Those peaks were previously considered as volcanic inputs. For example, the peaks in 1991–1992 were ascribed to the Cerro Hudson eruption in 1991 (Soyol-Erdene et al., 2011). This comparison did not provide any evidence of increased Hg sequestration by terrestrial dust, since both the low baseline and the intermittent peaks of Ba did not explain the increases of Hg_T.

Hg_T fluxes in 1987 and 1988 were much higher than expected from the Na^+ fluxes (two ourliers in Fig. 4b), suggesting that additional factors influenced the Hg sequestration rate. We propose that an increase of snow accumulation in summer can enhance the Hg sequestration by scavenging atmospheric Hg^{II} and burying deposited Hg^{II} below the photochemically active snow layer. The snow layers corresponding to 1987–1988 were characterized by summer-type features with the low Na^+ concentration, high Cl^-/Na^+ ratio and high $\delta^{18}O$ relative to neighboring layers. Another probable factor is the UV-B flux on the surface snow, which drives the photochemical reduction of Hg^{II} in snow: the greater the UV flux, the lower the Hg_T in snow (Dommergue et al., 2007; Mann et al., 2015). The surface UV flux is dependent on the ozone concentration in the atmosphere, especially in the stratosphere. For example, the UV-B flux was highly correlated to the total column ozone ($r = -0.92$, $p < 0.001$, 1997–2011) at Showa Station in September–October when the photochemistry is most active (Fig. S1; data from the JMA website, http://www.data.jma.go.jp/). The higher stratospheric ozone concentrations in the 1980s caused lower surface UV flux and consequently less reduction of Hg^{II} in the snow. We observed a considerable correlation between the total column ozone at Showa Station and the Hg_T flux at Dome Fuji ($r = 0.83$, $p < 0.001$). Meteorological conditions affect snow metamorphism that can change physical and chemical properties of snowpack and hence the UV flux below the surface (Domine et al., 2006). The degree to which the Hg dynamics depend on meteorological conditions and the UV flux must be further investigated.

4. Conclusion

The CV-ICP-SFMS technique provided satisfactory precision for resolving sub-annual variations in net Hg depositions recorded in the Dome Fuji snowpack. Although photochemical Hg exchange between the atmosphere and snowpack would occur throughout the sunlight period and be more active in mid to late summer, the snowpack did not show regular increases in the net Hg deposition during summer. The lack of summertime growth of the net Hg deposition confirmed that most of the deposited Hg was re-emitted over the course of the air-snow Hg exchange. The re-emission would be favored in the Antarctic Plateau since the slow snow accumulation allows enough time for the deposited Hg^{II} to be reduced within the photochemically active snow layer. The enhancement of the net Hg deposition occurred between late winter and early summer when the sea salt content in the snow was relatively high, and the annual deposition fluxes of Hg were positively related to those of Na^+. This relationship suggests the possibility

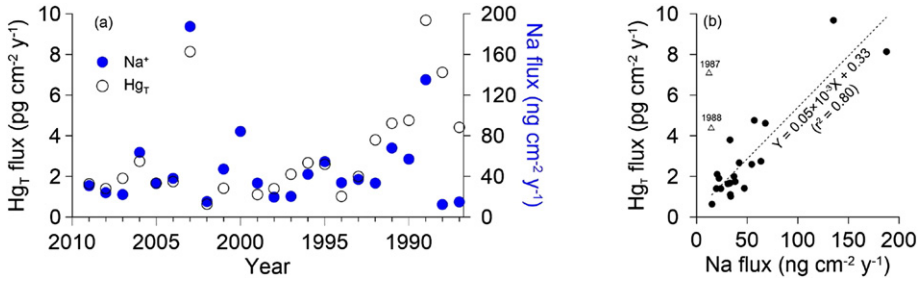

Fig. 4. (a) The annual fluxes of Hg_T (open circle) and Na^+ (closed circle) between 1987 and 2009 CE (b) The positive relationship ($r = 0.70$; $p < 0.001$) between the Hg_T and Na^+ fluxes, including two outliers (open triangle). The outlying points are excluded from the regression line (dotted line).

that part of the deposited Hg^{II} formed complexes with sea salt halogens and were bound to sea salt, and those were resistant to the photochemical reduction and perennially remained in the snowpack.

Acknowledgments

We thank all field personnel for sampling during the 51st Japanese Antarctic Research Expedition. This research was supported by the NRF Mid-Career Research Program (No. 2011-0015174) and the Basic Science Research Program (NRF-2014R1A1A3049836) funded by MSIP, research grants (PE16010 and PE17040) from the Korea Polar Research Institute (KOPRI), and the Japan Society for the Promotion of Science (JSPS) (research grant (A) 20241007).

Appendix A. Supplementary data

A supplementary data file includes a data table of Hg_T, Hg_L, major ion concentrations and $\delta^{18}O$ (Table S1) and the total ozone concentration and surface UV-B flux at Showa Station (Fig. S1). Supplementary data associated with this article can be found in the online version, at http://dx.doi.org/10.1016/j.scitotenv.2017.01.008.

References

Angot, H., Magand, O., Helmig, D., Ricaud, P., Quennehen, B., Gallée, H., Del Guasta, M., Sprovieri, F., Pirrone, N., Savarino, J., Dommergue, A., 2016. New insights into the atmospheric mercury cycling in central Antarctica and implications on a continental scale. Atmos. Chem. Phys. 16 (13), 8249–8264.

Bartels-Rausch, T., Huthwelker, T., Jöri, M., Äggeler, H.W., Ammann, M., 2008. Interaction of gaseous elemental mercury with snow surfaces: laboratory investigation. Environ. Res. Lett. 3 (4), 045009.

Boutron, C.F., 1995. Historical reconstruction of the earth's past atmospheric environment from Greenland and Antarctic snow and ice cores. Environ. Rev. 3 (1), 1–28.

Brooks, S., Arimoto, R., Lindberg, S., Southworth, G., 2008a. Antarctic polar plateau snow surface conversion of deposited oxidized mercury to gaseous elemental mercury with fractional long-term burial. Atmos. Environ. 42 (12), 2877–2884.

Brooks, S., Lindberg, S., Southworth, G., Arimoto, R., 2008b. Springtime atmospheric mercury speciation in the McMurdo, Antarctica coastal region. Atmos. Environ. 42 (12), 2885–2893.

Capelli, R., Minganti, V., Chiarini, C., Pellegrini, R.D., 1998. Mercury in snow layers from the Antarctica. Int. J. Environ. Anal. Chem. 71 (3–4), 289–296.

Domine, F., Taillandier, A.-S., Houdier, S., Parrenin, F., Simpson, W.R., Douglas, T.A., 2006. Interactions between snow metamorphism and climate: Physical and chemical aspects. Spec. Publ. R. Soc. Chem. 1, 311–327.

Dommergue, A., Bahlmann, E., Ebinghaus, R., Ferrari, C., Boutron, C., 2007. Laboratory simulation of Hg^0 emissions from a snowpack. Anal. Bioanal. Chem. 388 (2), 319–327.

Dommergue, A., Sprovieri, F., Pirrone, N., Ebinghaus, R., Brooks, S., Courteaud, J., Ferrari, C.P., 2010. Overview of mercury measurements in the Antarctic troposphere. Atmos. Chem. Phys. 10 (7), 3309–3319.

Dommergue, A., Barret, M., Courteaud, J., Cristofanelli, P., Ferrari, C.P., Gallée, H., 2012. Dynamic recycling of gaseous elemental mercury in the boundary layer of the Antarctic Plateau. Atmos. Chem. Phys. 12 (22), 11027–11036.

Durnford, D., Dastoor, A., 2011. The behavior of mercury in the cryosphere: a review of what we know from observations. J. Geophys. Res.-Atmos. 116, D06305.

Enomoto, H., Motoyama, H., Shiraiwa, T., Saito, T., Kameda, T., Furukawa, T., Takahashi, S., Kodama, Y., Watanabe, O., 1998. Winter warming over Dome Fuji, East Antarctica and semiannual oscillation in the atmospheric circulation. J. Geophys. Res.-Atmos. 103 (D18), 23103–23111.

Ferrari, C.P., Dommergue, A., Boutron, C.F., Jitaru, P., Adams, F.C., 2004. Profiles of mercury in the snow pack at Station Nord, Greenland shortly after polar sunrise. Geophys. Res. Lett. 31, L3401.

Fujita, K., Abe, O., 2006. Stable isotopes in daily precipitation at Dome Fuji, East Antarctica. Geophys. Res. Lett. 33, L18503.

Han, Y., Huh, Y., Hong, S., Hur, S.D., Motoyama, H., Fujita, S., Nakazawa, F., Fukui, K., 2011. Quantification of total mercury in Antarctic surface snow using ICP-SF-MS: spatial variation from the coast to Dome Fuji. Bull. Kor. Chem. Soc. 32 (12), 4258–4264.

Han, Y., Huh, Y., Hong, S., Hur, S.D., Motoyama, H., 2014. Evidence of air-snow mercury exchange recorded in the snowpack at Dome Fuji, Antarctica. Geosci. J. 18 (1), 105–113.

Hara, K., Osada, K., Kido, M., Hayashi, M., Matsunaga, K., Iwasaka, Y., Yamanouchi, T., Hashida, G., Fukatsu, T., 2004. Chemistry of sea-salt particles and inorganic halogen species in Antarctic regions: compositional differences between coastal and inland stations. J. Geophys. Res.-Atmos. 109, D20208.

Hong, S., Lluberas, A., Rodriguez, F., 2000. A clean protocol for determining ultralow heavy metal concentrations: its application to the analysis of Pb, Cd, Cu, Zn and Mn in Antarctic snow. Korean J. Polar Res. 11 (1), 35–47.

Hong, S., Soyol-Erdene, T.O., Hwang, H.J., Hong, S.B., Hur, S.D., Motoyama, H., 2012. Evidence of global-scale As, Mo, Sb, and Tl atmospheric pollution in the Antarctic snow. Environ. Sci. Technol. 46 (21), 11550–11557.

Hoshina, Y., Fujita, K., Nakazawa, F., Iizuka, Y., Miyake, T., Hirabayashi, M., Kuramoto, T., Fujita, S., Motoyama, H., 2014. Effect of accumulation rate on water stable isotopes of near-surface snow in inland Antarctica. J. Geophys. Res.-Atmos. 119 (1), 274–283.

Iizuka, Y., Fujii, Y., Hirasawa, N., Suzuki, T., Motoyama, H., Furukawa, T., Hondoh, T., 2004. SO_4^{2-} minimum in summer snow layer at Dome Fuji, Antarctica, and the probable mechanism. J. Geophys. Res.-Atmos. 109, D04307.

Iizuka, Y., Hondoh, T., Fujii, Y., 2008. Antarctic sea ice extent during the Holocene reconstructed from inland ice core evidence. J. Geophys. Res.-Atmos. 113, D15114.

Iizuka, Y., Tsuchimoto, A., Hoshina, Y., Sakurai, T., Hansson, M., Karlin, T., Fujita, K., Nakazawa, F., Motoyama, H., Fujita, S., 2012. The rates of sea salt sulfatization in the atmosphere and surface snow of inland Antarctica. J. Geophys. Res.-Atmos. 117, D04308.

Jitaru, P., Gabrielli, P., Marteel, A., Plane, J.M.C., Planchon, F.A.M., Gauchard, P.-A., Ferrari, C.P., Boutron, C.F., Adams, F.C., Hong, S., Cescon, P., Barbante, C., 2009. Atmospheric depletion of mercury over Antarctica during glacial periods. Nat. Geosci. 2 (7), 505–508.

JMA, d. Japan Meteorological Agency Website. http://www.data.jma.go.jp/gmd/env/ozonehp/diag_o3uv.html (accessed 16.09.05).

Kameda, T., Motoyama, H., Fujita, S., Takahashi, S., 2008. Temporal and spatial variability of surface mass balance at Dome Fuji, East Antarctica, by the stake method from 1995 to 2006. J. Glaciol. 54 (184), 107–116.

King, M.D., Simpson, W.R., 2001. Extinction of UV radiation in Arctic snow at Alert, Canada (82° N). J. Geophys. Res. 106 (D12), 12499–12507.

Li, C., Kang, S., Shi, G., Huang, J., Ding, M., Zhang, Q., Zhang, L., Guo, J., Xiao, C., Hou, S., Sun, B., Qin, D., Ren, J., 2014. Spatial and temporal variations of total mercury in Antarctic snow along the transect from Zhongshan Station to Dome A. Tellus B. 66, p. 25152.

Mann, E., Ziegler, S., Mallory, M., O'Driscoll, N., 2014. Mercury photochemistry in snow and implications for Arctic ecosystems. Environ. Rev. 22 (4), 331–345.

Mann, E.A., Mallory, M.L., Ziegler, S.E., Tordon, R., O'Driscoll, N.J., 2015. Mercury in Arctic snow: quantifying the kinetics of photochemical oxidation and reduction. Sci. Total Environ. 509-510, 115–132.

Massom, R.A., Pook, M.J., Comiso, J.C., Adams, N., Turner, J., Lachlan-Cope, T., Gibson, T.T., 2004. Precipitation over the interior East Antarctic ice sheet related to midlatitude blocking-high activity. J. Clim. 17 (10), 1914–1928.

Motoyama, H., Hirasawa, N., Satow, K., Watanabe, O., 2005. Seasonal variations in oxygen isotope ratios of daily collected precipitation and wind drift samples and in the final snow cover at Dome Fuji Station, Antarctica. J. Geophys. Res.-Atmos. 110, D11106.

Nerentorp Mastromonaco, M., Gårdfeldt, K., Jourdain, B., Abrahamsson, K., Granfors, A., Ahnoff, M., Dommergue, A., Méjean, G., Jacobi, H.-W., 2016. Antarctic winter mercury and ozone depletion events over sea ice. Atmos. Environ. 129, 125–132.

Pfaffhuber, K.A., Berg, T., Hirdman, D., Stohl, A., 2012. Atmospheric mercury observations from Antarctica: seasonal variation and source and sink region calculations. Atmos. Chem. Phys. 12, 3241–3251.

Planchon, F.A.M., Gabrielli, P., Gauchard, P.A., Dommergue, A., Barbante, C., Cairns, W.R.L., Cozzi, G., Nagorski, S.A., Ferrari, C.P., Boutron, C.F., Capodaglio, G., Cescon, P., Varga, A., Wolff, E.W., 2004. Direct determination of mercury at the sub-picogram per gram level in polar snow and ice by ICP-SFMS. J. Anal. At. Spectrom. 19 (7), 823–830.

Rankin, A.M., Wolff, E.W., Martin, S., 2002. Frost flowers: implications for tropospheric chemistry and ice core interpretation. J. Geophys. Res.-Atmos. 107 (D23), 4683.

Schlosser, E., Manning, K.W., Powers, J.G., Duda, M.G., Birnbaum, G., Fujita, K., 2010. Characteristics of high-precipitation events in Dronning Maud Land, Antarctica. J. Geophys. Res.-Atmos. 115, D14107.

Sherman, L.S., Blum, J.D., Johnson, K.P., Keeler, G.J., Barres, J.A., Douglas, T.A., 2010. Mass-independent fractionation of mercury isotopes in Arctic snow driven by sunlight. Nat. Geosci. 3 (3), 173–177.

Soyol-Erdene, T.-O., Huh, Y., Hong, S., Hur, S.D., 2011. A 50-year record of platinum, iridium, and rhodium in Antarctic snow: volcanic and anthropogenic sources. Environ. Sci. Technol. 45 (14), 5929–5935.

Suzuki, T., Iizuka, Y., Matsuoka, K., Furukawa, T., Kamiyama, K., Watanabe, O., 2002. Distribution of sea salt components in snow cover along the traverse route from the coast to Dome Fuji station 1000 km inland at east Dronning Maud Land, Antarctica. Tellus B 54 (4), 407–411.

Takahashi, S., Kameda, T., 2007. Snow density for measuring surface mass balance using the stake method. J. Glaciol. 53 (183), 677–680.

Udisti, R., Dayan, U., Becagli, S., Busetto, M., Frosini, D., Legrand, M., Lucarelli, F., Preunkert, S., Severi, M., Traversi, R., Vitale, V., 2012. Sea spray aerosol in central Antarctica. Present atmospheric behaviour and implications for paleoclimatic reconstructions. Atmos. Environ. 52, 109–120.

US EPA, United State Environmental Protection Agency, 2005. Method 245.7 mercury in water by cold vapor atomic fluorescence spectrometry, EPA-821-R-05-001. http://nepis.epa.gov/Exe/ZyPDF.cgi/P1008IY8.PDF?Dockey=P1008IY8.PDF (accessed 16.09.05).

Vandal, G.M., Fitzgerald, W.F., Boutron, C.F., Candelone, J.-P., 1993. Variations in mercury deposition to Antarctica over the past 34,000 years. Nature 362, 621–623.

Witherow, R.A., Lyons, W.B., 2008. Mercury deposition in a polar desert ecosystem. Environ. Sci. Technol. 42 (13), 4710–4716.

Wolff, E.W., Fischer, H., Fundel, F., Ruth, U., Twarloh, B., Littot, G.C., Mulvaney, R., Röthlisberger, R., de Angelis, M., Boutron, C.F., Hansson, M., Jonsell, U., Hutterli, M.A., Lambert, F., Kaufmann, P., Stauffer, B., Stocker, T.F., Steffensen, J.P., Bigler, M., Siggaard-Andersen, M.L., Udisti, R., Becagli, S., Castellano, E., Severi, M., Wagenbach, D., Barbante, C., Gabrielli, P., Gaspari, V., 2006. Southern Ocean sea-ice extent, productivity and iron flux over the past eight glacial cycles. Nature 440 (7083), 491–496.

Yang, X., Pyle, J.A., Cox, R.A., 2008. Sea salt aerosol production and bromine release: role of snow on sea ice. Geophys. Res. Lett. 35, L16815.